

Simulation Study of Capacitance Tomography Sensors

Hua Yan, Fuqun Shao, and Shi Wang

School of Information Science & Engineering,
 P. O. Box 321, Northeastern University, Shenyang, 110006, P. R. China,
 e-mail: cxscxsc@pub.sy.ln.cn

Abstract:- ECT sensors can be divided into three types according to their axial guard electrode design. Type 1: with earthed ring guards; type 2: with driven segmented guards and type 3: without guards. In this paper, the axial sensitivity distribution, and hence the effective measurement space of above three ECT sensors are analysed using three dimensional finite element method. Analysis shows that the effective measurement space of type 1 is the narrowest in axial direction, and that of type 2 is the widest. This result is confirmed by reconstructed images. Finally, which type ECT sensor is suitable for imaging a blast furnace is discussed. Due to the furnace burden is axial layered, limiting the effective measurement space is essential to the reconstruction image quality.

Keywords: ECT sensor, effective sensing space, sensor structure, simulation

1. INTRODUCTION

Electrical capacitance tomography (ECT) has been developed to image industrial processes containing dielectric materials, e.g., gas/oil flows in oil pipelines, gas/solid flows in pneumatic conveyors and fluidization processes in fluidized beds[1]. An ECT sensor consists of multiple measurement electrodes mounted equally around the cross section of a process to be imaged, with an earthed screen outside the measurement electrodes to reject external noise (see Figure1). The capacitances of all possible electrode combinations are measured and used to reconstruct a cross-sectional image (i.e. the permittivity distribution) using a reconstruction algorithm, for example, filtered linear back-projection algorithm[2].

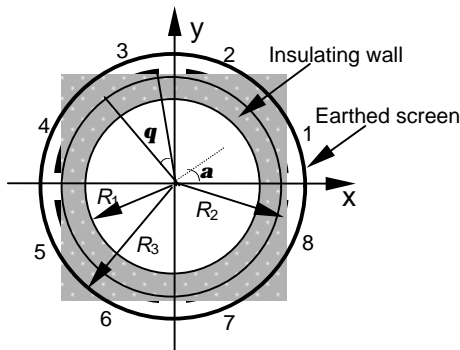


Figure1: Arrangement of measurement electrodes of an 8-electrode ECT sensor

ECT sensors can be divided into three types according to their axial guard electrode design: type 1: ECT sensor with two earthed ring guard electrodes above and below the measurement

electrodes; type 2: with two sets of driven segmented guard electrodes and type 3 without guard electrodes. These three types ECT sensors are shown schematically in Figure2. For simplicity, the earthed screen is not shown in Figure 2.

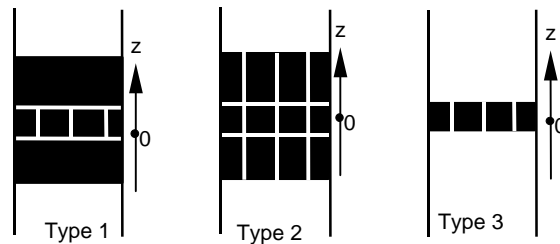


Figure2. Three types ECT sensors.

The sensing field of an ECT sensor is non-uniform distributed in a three-dimensional space, the data obtained from the ECT system reflect the medium distribution in a relatively large space. Therefore, in order to give a physical meaning to the reconstructed images, it is necessary to improve the axial evenness of the sensing field and focus its effective measurement space. The guard design of ECT sensor, no doubt has an important influence on the sensing field distribution, and on the reconstructed image quality.

Using a three-dimensional finite element (FE)method software package developed for the simulation study of ECT system by the authors, the three dimensional sensing field of above three types ECT sensors are analysed. The axial sensitivity distribution and the effective sensing space is mainly concerned.

Finally, which type ECT sensor is suitable for imaging a blast furnace is discussed in this paper. Imaging a blast furnace is quite different from imaging pipe flows. The diameter of a blast furnace is as great as several meters and the furnace burden is axial layered, so the ratio between the axial measurement electrode length and the blast furnace diameter is small. More than that, long guard electrodes are not permissible.

2. 3D FINITE ELEMENT MODEL OF ECT SENSOR

The electrostatic field in the capacitance sensor is governed by Laplace's equation (assuming free space charge distribution inside the screen):

$$\nabla \cdot (\epsilon(x,y,z)\nabla\phi(x,y,z)) = 0 \quad (1)$$

The solution of this equation under proper boundary conditions (the Dirichlet conditions) by FE method gives nodal potential values, from which capacitance between any pair of electrodes and subsequently the sensor sensitivity can be calculated.

One of the advantages with FE method is that the shapes of the elements can vary from element to element, and they can therefore be put together to represent complex geometry. In general, the shapes of the elements are intentionally made as simple as possible, such as triangle and quadrilateral elements in two-dimensional domains, and tetrahedra, pentahedra, and hexahedra elements in three dimensional domains.

In our ECT sensor models, 8 node hexahedra and 6 node pentahedra elements are used for 3 dimensional meshing. Figure 3 is a finite element mesh in the base plane of an 8-electrode ECT sensor. The 3D mesh is extruded in the third dimension (Z direction) on the base plane with the finer subdivision around the electrodes.

3. SENSITIVITY DISTRIBUTION AND ITS OBTAINING METHODS

The sensitivity distribution of electrode pair $i-j$, $S_{i,j}(k)$ can be defined as:

$$S_{i,j}(k) = \frac{C_{i,j}(k) - C_{i,j}^l}{C_{i,j}^h - C_{i,j}^l} \frac{1}{\epsilon_h - \epsilon_l} \mu(k) \quad (2)$$

$i=1,2,\dots,7, j=i+1,\dots,8$

where ϵ_l and ϵ_h are respectively the permittivities of the high permittivity material and the low permittivity material. $C_{i,j}(k)$ is the capacitance of electrode pair $i-j$ when the k th

element inside the sensing space has permittivity ϵ_h and the rest of the elements inside the sensing space all have permittivity ϵ_l . $C_{i,j}^l$, $C_{i,j}^h$ are the capacitances when the sensing space is filled with material of permittivity ϵ_l and ϵ_h respectively, $\mu(k)$ is a correction factor related to the volume of element k $\mu(k)$ has different values for elements of different volume.

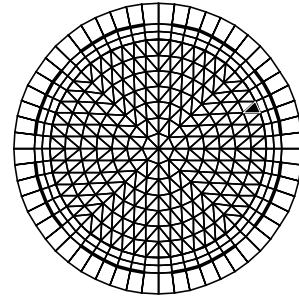


Figure3: Mesh in the base plane of an 8-electrode ECT sensor

In 2D analysis, the sensitivity distribution is essentially a map of the sensor response to a small individual area of high permittivity material in a low permittivity background as it positioned throughout the sensing area. Correspondingly, in 3D analysis, a small individual volume of high permittivity material in a low permittivity background as it positioned throughout the sensing volume.

The sensitivity distributions (or maps) can be obtained by physical measurement or by finite element (FE) analysis. There are several disadvantages difficult to overcome with the measurement method: (i) Many measurements are required; (ii) The test set up requires modification to investigate any change in physical parameters; (iii) The number of measurement points are rather limited for the test probe size must be big enough to ensure the capacitance changes are detectable; (iv) It is very difficult to position a short test probe in a certain position in the 3D sensing field and not bring influence to the measurement.

Consequently most investigators prefer the calculation method using a FE software package. The calculation of sensitivity maps is time consuming, especially in 3 dimension. To solve this problem, we adopted a fast calculation method of sensitivity distributions proposed by authors in reference[3]. This method is based on finite element method, by fast generation of global system matrix and fast calculation of capacitances, the consuming time of sensitivity distributions is reduced dramatically, and hence the 3D sensitivity distributions of an ECT sensor can be obtained conveniently.

4. AXIAL SENSITIVITY DISTRIBUTION OF ECT SENSORS

When the three dimensional sensitivity distribution is obtained, both the sensitivity distribution against x and y at a fixed z position, and the sensitivity distribution against z at a fixed x and y position can be easily plotted. Since it is more convenient to illustrate the axial (z-direction) distribution in two than three dimensional plots, and since the axial distribution is mainly concerned in this paper, a fixed x and y position is selected and marked in Figure 3 by black. Picking on this position is mainly because all the four typical electrode pairs (e.g. electrode pair 1-2,1-3,1-4 and 1-5) are sensitive to this position, and therefore, the axial sensitivity distribution at this position is representative.

According to the experimental model for blast furnace, the simulation of this paper is under following parameters: $R1=10.5\text{cm}$, $R2=12\text{cm}$, $R3=14\text{cm}$, $\theta=32.14^\circ$ (see Figure1). The permittivity of insulating wall is 8. The high and low permittivity in Equation 2 are $\epsilon_h=3$ and $\epsilon_l=1$ respectively.

Usually, for a fixed x and y position, the sensitivity at $z=0$ (the axial centre of electrodes, see Figure 2) is maximal, and the sensitivity attenuates with the increase of $|z|$. Therefore, the decrease degree of sensitivity at different z position relative to the sensitivity at $z=0$ can illustrate the axial sensitivity distribution conveniently. Using this method, the axial sensing distribution of the three types ECT sensors are investigated in following.

4.1 ECT sensor with earthed ring guard

Type 1 ECT sensor is with two earthed ring guard electrodes above and below the measurement electrodes, see Figure 2. For this type ECT sensor, the axial sensitivity attenuation curve shapes of the four typical electrode pairs are very similar, so only the curves of the adjacent electrode pair 1-2 are given.

The gap between the measurement and the guard electrodes has some influence on the axial sensitivity attenuation. The narrower the gap, the narrower the effective sensitivity space, see Figure 4. In figure 4 the gap is 0.15, 0.5, 1, 2, 4cm and infinite respectively and the axial length of the measurement and guard electrodes are fixed at 5 and 3cm respectively.

When the axial length of the ring guard electrodes is not short than 1cm, the axial sensitivity attenuation is not sensitive to the variance of the ring length, see Figure 5. In Figure 5 the axial length of guards is 0, 1, 3, 5cm and infinite respectively, and the axial length of

the measurement electrodes and the gap are fixed at 5 and 0.15cm respectively.

Increasing the axial length of the measurement electrodes, the sensitivity space will be expanded correspondingly, see Figure 6. In Figure 6 the axial length of measurement electrodes is 3, 5 and 7cm respectively, the gap and the axial length of the guard are fixed at 0.15cm and 3cm respectively.

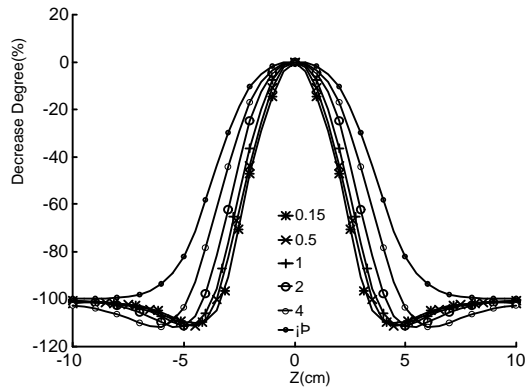


Figure4: Influence of the gap on the sensing field of electrode pair 1-2 for type 1 ECT sensor

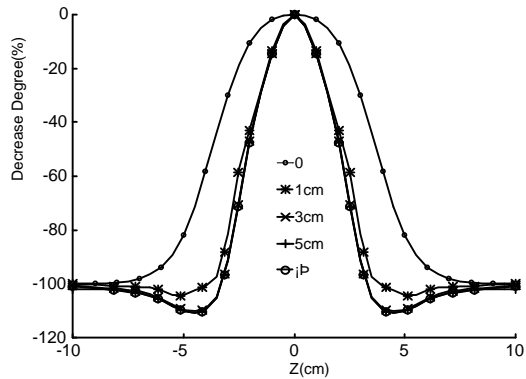


Figure5: Influence of the guard length on the sensing field of electrode pair 1-2 for type 1 ECT sensor

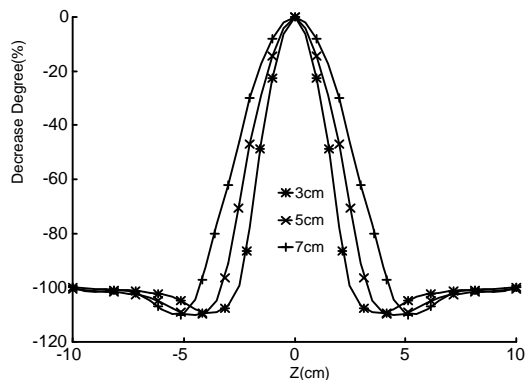


Figure6: Influence of the measurement electrode axial length on the sensing field of electrode pair 1-2 for type 1 ECT sensor

4.2 ECT sensor with driven segmented guard

Type 2 ECT sensor is with two sets of driven segmented guard electrodes above and below the measurement electrodes, see Figure 2. The segmented guard electrodes are as large in the circumferential direction as the measurement electrodes. Same potentials are applied to the guards and the corresponding measurement electrodes simultaneously.

For type 2 ECT sensor, The shapes of the axial sensitivity attenuation curve of the four typical electrode pairs are different, so the curves of adjacent electrode pair 1-2 and opposite electrode pair 1-5 are given.

The gap between the measurement and the guard electrodes has notable influence on the axial sensitivity attenuation and evenness, see Figure 7 and Figure 8, where the gap is 0.1, 0.5, 1 and 2cm respectively and the axial length of the measurement and guard electrodes are fixed at 5 and 3cm respectively. The narrower the gap, the narrower the effective sensitivity space. A wide gap will degrade the evenness of the effective sensing field remarkably. So the three planes of electrodes should be mounted as physically close as possible.

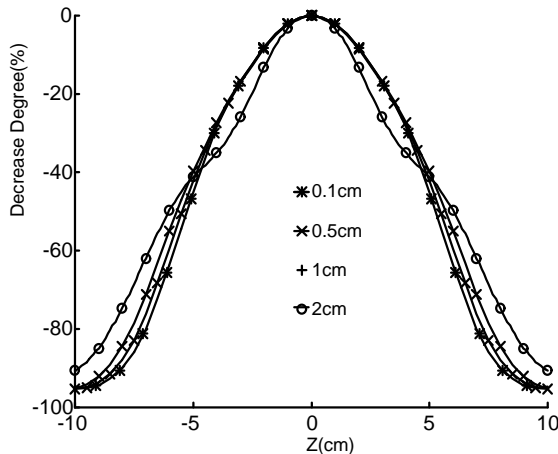


Figure7: Influence of the gap on the sensing field of electrode pair 1-2 for type2 ECT sensor

When the guard axial length is shorter than 6cm, the enlargement of the effective sensing space with the increase of the guard length is remarkable. However, when the guard length is longer than 6cm, the change of effective sensing space with the increase of the guard length is little, see Figure 9 and Figure 10. In Figure9,10 the axial length of guard electrodes is 1, 3, 5, 6cm and infinite respectively, the axial length of the measurement electrodes and the gap are fixed at 5 and 0.1cm respectively.

Increasing the axial length of the measurement electrodes, the sensitivity space will be expanded correspondingly, see Figure 11 and Figure 12, where the axial length of measurement electrodes is 3, 5 and 7cm

respectively, the gap and the axial length of the guard are fixed at 0.1cm and 3cm respectively.

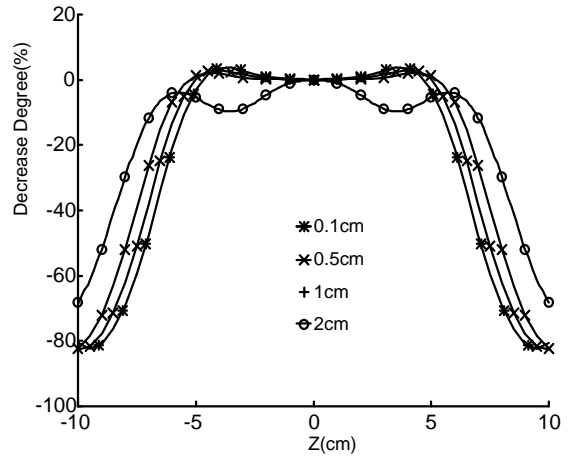


Figure8: Influence of the gap on the sensing field of electrode pair 1-5 for type 2 ECT sensor

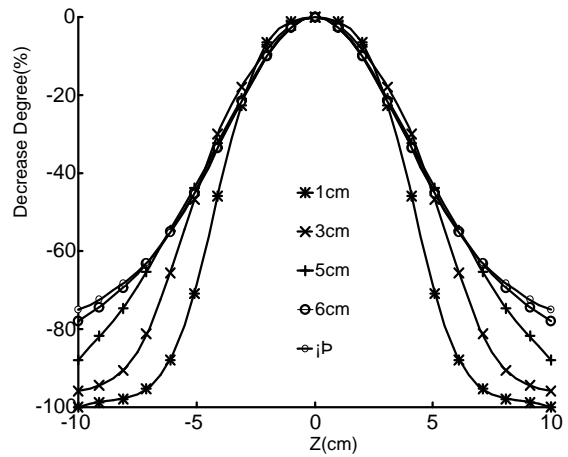


Figure9: Influence of the guard length on the sensing field of electrode pair 1-2 for type 2 ECT sensor

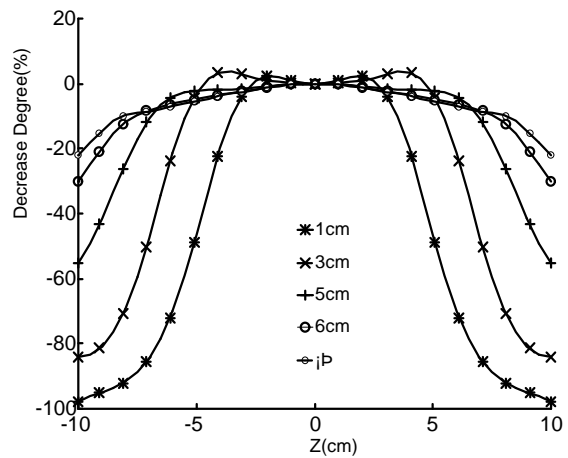


Figure10: Influence of the guard length on the sensing field of electrode pair 1-5 for type 2 ECT sensor

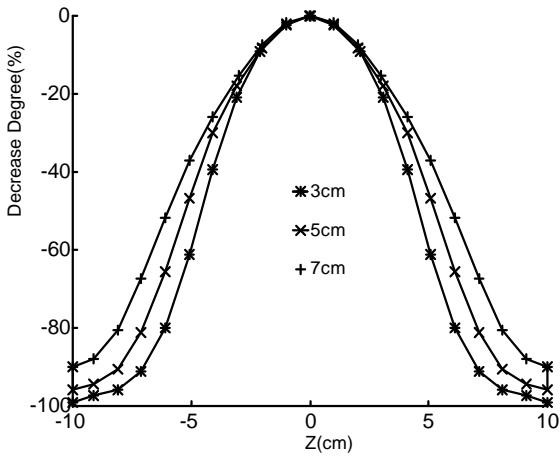


Figure11: Influence of the measurement electrode axial length on the sensing field of electrode pair 1-2 for type 2 ECT sensor

distribution on this plane for empty type 1, 2 and 3 ECT sensor are shown in Fig 14, 15 and 16 respectively.

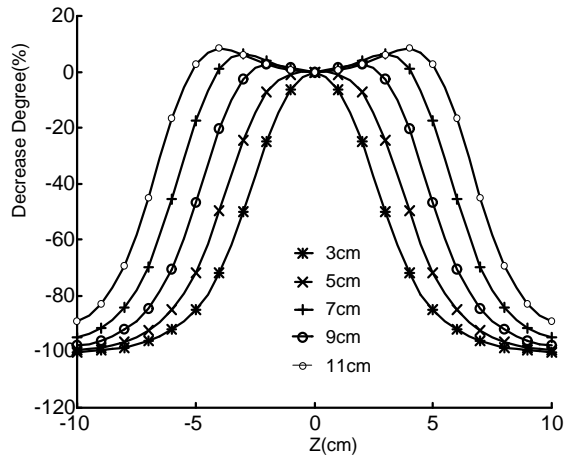


Figure13: Influence of the measurement electrode axial length on the sensing field of electrode pair 1-2 for type 3 ECT sensor

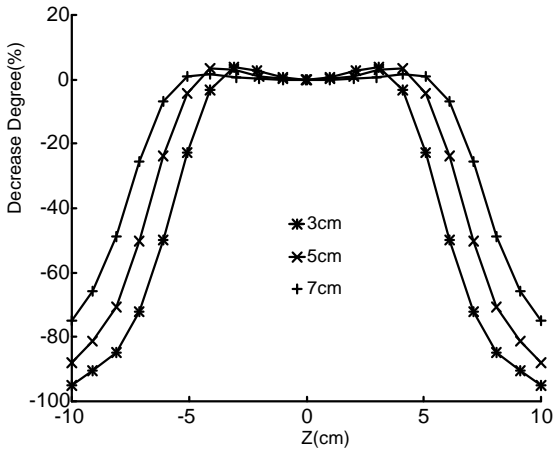


Figure12: Influence of the measurement electrode axial length on the sensing field of electrode pair 1-5 for type 2 ECT sensor

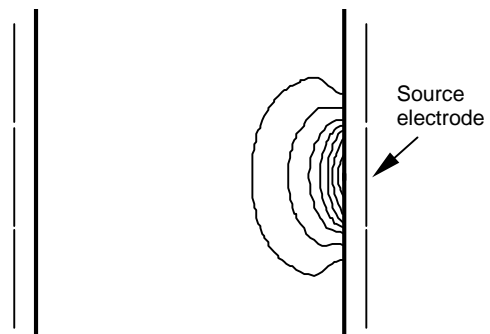


Figure14: potential distribution on plane $\alpha = 22.5^\circ$ for empty type 1 ECT sensor

4.3 ECT sensor without guard electrodes

Type 3 ECT sensor is without guard electrodes, see Figure 13. For this type ECT sensor, the axial sensitivity attenuation curve shapes of the four typical electrode pairs are very similar, so only the curves of adjacent electrode pair 1-2 are given.

The greater the axial length of the electrode, the larger the effective sensing field, this can be seen from Figure 13, where the axial length of the measurement electrodes is 3, 5, 7, 9, 11cm respectively.

5 POTENTIAL DISTRIBUTION FOR EMPTY ECT SENSORS

The potential distribution on a special section plane (the plane defined by $\alpha = 22.5^\circ$ see Figure 1) is selected to analyse the potential distribution inside the insulating wall. The potential

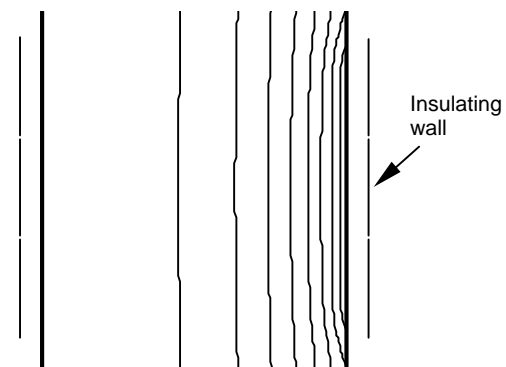


Figure15: potential distribution on plane $\alpha = 22.5^\circ$ for empty type 2 ECT sensor

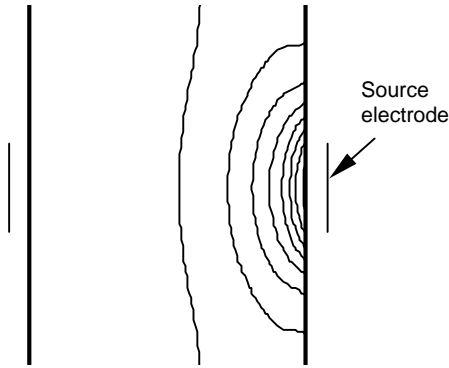


Figure16: potential distribution on plane $\alpha = 22.5^\circ$ for empty type 3 ECT sensor

For convenience in discussion, the column enclosed by the measurement electrodes is called region M and by the guards region G. Obviously, for type 3 and notable for type 1 ECT sensor, the electric field in region G is rather weak, and rapidly diminishing in magnitude with the increase of $|z|$. However for type 2 ECT sensor, the equipotential counters are basically parallel to the z-axes in region M and G. The electric field in region G is nearly as strong as that in region M.

When a high permittivity volume presents in region G, the polarisation charges produced will affect the electric field distribution in region M and hence change the measurement capacitance values since the capacitance sensor is a 'soft' sensor. The stronger the electric field, the more the polarisation charges produced, and the more change of the capacitance values.

Since the influence of the polarisation charges produced in region G on the electric field in region M diminishes with the increase of the distance to the region M, the effective sensing space will include region M and partial or entire region G, depending on the size of region G. This can be seen in section 4.2. So the effective sensing space of type 2 ECT sensor is the widest.

A point which is especially to be noted is that the equipotential counters for a non-empty type 2 ECT sensor is not parallel any more, unless the high permittivity material distribution does not change spatially along the axial direction, at least within region M and region G.

In this section and the following section (i.e. section 6), the axial length of the measurement electrodes is fixed at 5cm, no matter for type 1, 2 or 3 ECT sensor. The axial length of guard electrodes and the gap between the measurement and the guard electrodes for type 1 is 5cm and 0.15cm, and that for type 2 is 5cm and 0.1cm.

6 ASSESSMENT ON THE SENSING VOLUME BY RECONSTRUCTED IMAGES

From the axial sensitivity distributions presented in section 4, it can be found that for the same set of measurement electrodes, the effective sensing space of type 1 is the narrowest in axial direction, and that of type 2 is the widest. To conform this, image reconstruction tests were carried out by further simulation using the sensitivity maps obtained at $z=0$ and the filtered linear back-projection algorithm.

Two phantoms were constructed by finite element method. For each phantom, two 'objects', named 'object' 1 and 'object' 2 were situated in different axial position. see Figure 17.

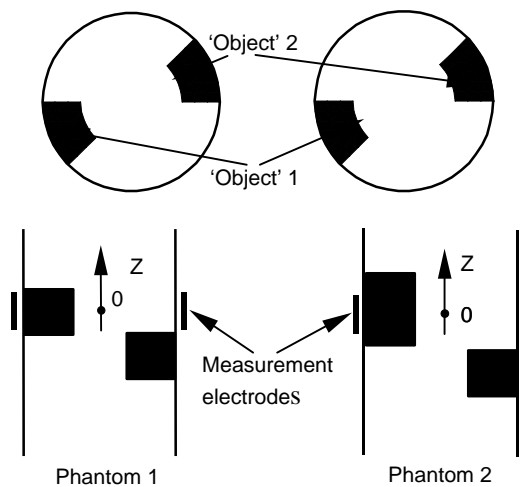


Figure17: two phantoms for image reconstruction tests

The reconstruction images are shown in Figure 18. Whether 'object' 2 appears in the reconstructed image can be used to assess the effective sensing space in z-direction. Obviously, type 1 poses the narrowest space, and type 2 the widest.

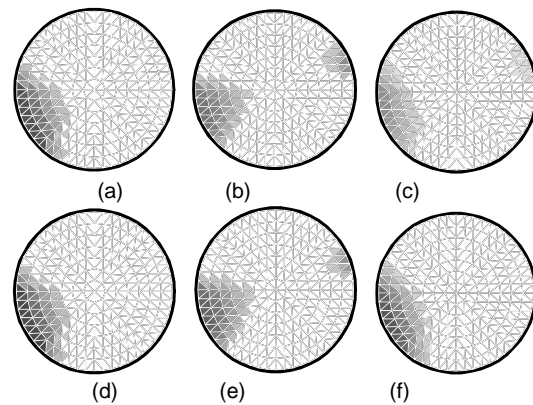


Figure 18: reconstructed images of phantom1 and 2 with type 1, 2 and 3 ECT sensor
 (a)phantom 1, type 1 (d)phantom 2, type 1
 (b)phantom 1, type 2 (e)phantom 2, type 2
 (c)phantom 1, type 3 (f)phantom 2, type 3

7 CONCLUSION AND DISCUSSION

Using the three dimensional finite element method, the sensing field of the three types ECT sensors are investigated. Several conclusions can be drawn as follows:

(1) For the same set of measurement electrodes, the size of effective sensing space is determined by sensor type. Type 1 ECT poses the narrowest in axial direction and type2 the largest.

(2) For each type ECT sensor, the effective sensitivity space will be expanded correspondingly with the increase of the axial length of the measurement electrodes. .

(3) For type 1 ECT sensor, the earthed ring guard pose a strong sink for electric fields, so its effective sensing space is rather narrow, within the column enclosed by the measurement electrodes (region M). The narrower the gap between the measurement and the guard electrodes, the narrower the effective sensitivity space. When the guard length exceeds a certain value, the axial sensitivity attenuation is not sensitive to the variance of the ring length.

(4) For type 2 ECT sensor, the driven segmented guard pose a rather strong electric field in the region enclosed by the guard (region G), so the effective sensing space is much wider than the size of region M. The effective sensing space will include region M and partial or entire region G, depending on the size of region G. The gap between the measurement and the guard electrodes has notable influence on the axial sensitivity attenuation and evenness, the three planes of electrodes should be mounted as physically close as possible.

(5) For type.3 ECT sensor, the effective sensing space is a few larger than the size of region M.

The advantage of type 1 ECT sensor consist in its narrow sensing space, and besides, the earthed ring guards can be used to protect the electrodes from the interference of external electrical fields. The disadvantage of type 1 ECT sensor is the small standing capacitance (the capacitance when the sensor is empty). For example, when the measurement electrode axial length is 5cm, the standing capacitance of adjacent electrode pair for type 3 ECT sensor (without guard electrodes) is 2.228pF, and the standing capacitance for a type 3 ECT sensor with the gap of 0.15cm, the ring length of 3cm is only 1.037pF.

In the situation where the component distribution does not change spatially along the axial direction (at least within the sensor effective sensing space), type 2 ECT sensor is a good choice and the sensing field can be simplified as a two dimensional electrical field. When the component distribution is quite different in axial

direction, type 2 ECT sensor is usually not a good choice for its large effective sensing space. Another inconvenience of type 2 is the complex in physical realisation

Type 3 is the simplest In physical realisation..

Owing to the furnace burden is axial layered, limiting the effective measurement space is essential to the reconstruction image quality. Based above analysis, the conclusion that type1 ECT sensor is suitable for imaging a blast furnace can be made naturally.

ACKNOWLEDGEMENT

The authors wish to thank the National Nature Science Foundation of China for financially supporting this research under contract No. 59674016.

REFERENCES

- [1] R. Mann and M. Wang, "Electrical process tomography: Simple and inexpensive techniques for process imaging", *Measurement and Control*, 1997, 30, pp.206-211.
- [2] C.G. Xie, S.M. Huang, B.S.Hoyle, and et al, "Electrical capacitance tomography for flow imaging: system mode for development of image reconstruction algorithms and design of primary sensors", *IEE proceeding-G*, 1992, 139, pp89-98.
- [3] H. Yan, F.Q. Shao and S. Wang, "Fast calculation of sensitivity distributions of capacitance tomography sensors", *Electronics Letters*, 1998, 34,1936-1937